

Stress concentration factor based design curves for cylinder-cylinder connections in pressure vessels

Murat Bozkurt^{1*}, David Nash²

¹Department of Mechanical Engineering, İstanbul University – Cerrahpaşa

²Department of Mechanical and Aerospace Engineering, University of Strathclyde

Abstract: The results of the parametric analysis of the cylinder-cylinder intersections in pressure vessels, performed in both elastic and plastic regions, are discussed in this study. Besides, the outcomes that contribute to the development of classical solutions in the literature are addressed as design curves depending on stress concentration factors (SCF). To begin with, the maximum stresses for cylinder-cylinder connections were calculated by finite element analysis, and SCF values were obtained. In these calculations, external local loads acting on the nozzle center and internal pressure are the main variables for loading conditions. Following that, different parametric approaches and loading conditions are presented to develop design curves for cylinder/cylinder connections by changing the main geometric parameters, such as cylinder and nozzle radii, and their thicknesses. A new approach is presented using these new curves thus allowing industrial designers to calculate maximum nozzle stresses without the need to undertake a thorough finite element analysis.

Keywords: Pressure Vessel, Stress Concentration Factors, Nozzle, FEA, Design Curves

1. Introduction

There is a significant difference in difficulty between analyzing sphere/cylinder intersections and cylinder/cylinder geometry in pressure vessel problems. The literature presents a number of theoretical solutions; however, until now, none have been implemented into an industrial code of practice, since these contain assumptions and restrictions that can impose severe limitations on the solutions. For instance, when it is desired to calculate the SCF for a cylindrical vessel-nozzle connection, the existing calculation approach for the spherical vessel-nozzle connection could be used. [1]. There are some applications where sphere/cylinder models are used to determine hoop stresses in cylinder/cylinder models. In one approach, it is ensured that the remote membrane stress occurring on the sphere is equalized to the cylindrical container hoop stress. Another approach states that the radius of the cylindrical container should be 1.5 times smaller than the radius of the spherical container [2]. Stress distributions in cylinder/nozzle connections, however, are quite different from those obtained for sphere/nozzle connections once detailed stress distributions are obtained. Taking all this into account, it is considered necessary to provide designers with stress concentration factor design curves that contain several geometric parameters that can be easily accessed and directly provide physically representative solutions in the analysis of cylinder/cylinder problems.

Kharat et al. [3] obtained stress concentration factors originating from nozzle combinations in their study. The authors, using the finite element method to find the SCF, have used different computational approaches in the literature for the reliability of the results. A comparison case study is presented by changing parameters such as radius and wall thickness for the nozzle-vessel junction under constant internal pressure. As a result, it was observed that the results of FEA and the results obtained from the experimental data largely overlapped. Apart from that, this study also discusses how conservative the equations developed by Money [4], Moffat [5,6], Mershon [7], Peterson, Lind [8], and Decock [9] are in calculating SCF.

Kihui et al. [10], worked on cylinders with cross holes to calculate the SCF values. The main parameter considered here was the chamfer angle and length. In addition, the authors examined the thickness and radius ratios that created SCF values for these various combinations. As a result, the authors presented optimum chamfer angle values, which is helpful in those cases.

Mukhtar [11], on the other hand, carried out a comprehensive SCF assessment for 150 cases in nozzle-vessel connections. The authors developed a functional dimensionless expression for basic geometry ratios. In this way, they provided an improvement for the traditional empirical expression derivation. In addition, the limitations of

* Corresponding author.
Email: murat.bozkurt@iuc.edu.tr



the widely used p -SCF charts and their significant differences in certain points according to the cases examined are noted.

Besides, Gerdeen [12] used thin-walled vessels with side holes and crossholes to calculate the SCF. The main parameters for the SCF in the study were the ratio of the outside diameter to the hole diameter (outside diameter-to-bore diameter) and the ratio of the hole diameter to the bore diameter-to-sidehole diameter. This study is also useful as it includes shear effects in the solutions, which were neglected in previous studies. The obtained results were confirmed by comparing them with the experimental data in the literature.

In his study, Moffat [5] conducted a study to develop an equation for calculating the effective stress factor (ESF). Therefore, existing design curves are combined with experimental data, internal pressure loading, and external moment loading. Here the author used the term ESF to avoid confusion, as the term stress intensity factor (SIF) has a different definition, especially in piping systems and fracture mechanics. The results obtained are in accordance with ASME III rules, FEA results, and additional test results. In their other study [6], Moffat et al. tried to generate a correlation equation on the ESF results for cylinder-cylinder connections under internal pressure. The produced Effective Stress Factor magnitudes are well above the values obtained from the Finite Element Analysis calculation, and therefore ESF obtained can only be used with some confidence for the stress magnitudes of the crotch corner.

Nziu and Masu [13] tried to optimally determine the position of circular cross holes in thick-walled vessels. For this purpose, cross-drilled vessels for variable offset positions were examined. Thickness ratios were kept between 1.4 – 3.0. The results clearly demonstrate the variation of SCF with an offset of circular holes. With these SCF values, it is stated that the optimum offset value will be 0.9 for the specified ranges.

Moreover, Makulsawatudom et al.[14] reveal SCF values for thick cylindrical containers with circular and elliptical cross holes in their work. The main problem here is the way the holes intersect (plain, chamfered, and blend radiused).

In addition to these studies, Kharat and Kulkarni[15] categorize the studies on the stress intensity factors occurring in the pressure vessel openings and put forward a review article for the literature. Although the studies discussed are limited in number, they have been a guide for researchers who want to have information about the literature.

In this study, SCF values for a β coefficient determined depending on the problem type were obtained according to the parameters t/T , dm/Dm , D/T , di/Di , and Dp/dm . These curves for internal pressure, external loading,

and pad reinforcement serve as an alternative guide for researchers [16].

2. The Curve-Generating Process For Nozzle-Cylinder Connection Problems

The estimation of the maximum stress is the most crucial stage in determining the stress concentration variables. The opening where the nozzle is penetrated is the area where the stress concentration is most intense. Therefore, in the nozzle/cylinder junction areas, the inner crotch wall is where potentially the highest stress is expected under internal pressure loading conditions. On the other hand, estimations cannot be made about the maximum stress location and stress distributions for nozzle/cylinder connections without determining the direction and magnitude of the applied force at nozzle centripetal external loadings. In their earlier work [16, 17, 18], the authors validated the finite element model linked to the aforementioned scenarios. Due to this, solutions from finite element analysis are used in this section to compute the maximum stress belonging to external local loads and inner pressure. Also, the results are taken into account independent of the stress locations such as crotch corner or nozzle wall, etc. Outcomes are provided in the following SCFs:

$$\text{SCF} = (\text{Maximum calculated stress in cylinder}) / (\text{membrane stress}).$$

The membrane stress is $PD/2T$ for internal pressure loading and $V/2\pi r t$ for external local loading. The maximum stress values are taken from the FEA results.

At first, internal pressure loading conditions in nozzle-cylinder connections are examined under various parameters, and design curves are created. Reinforcement plate application will not be included in this section. The effect of the pad reinforcement is then looked at thereafter. Design curves for external local loads are generated in the third stage. Using the proper attachment parameter - β , all of these SCF data are shown.

Bijlaard's work will be taken as basis for attachment parameter- β . Basically, appropriate geometric parameters are recommended for nozzle and cylindrical connections according to the nozzle type (Round Attachment, Square Attachment). Since the subject of this study is cylinder-cylinder connections, the Round Attachment parameter was used. The most important parameters affecting the maximum stress in cylinder-cylinder intersection problems are the radii of the main cylinder and the nozzle. For this reason, the ratio of these two expressions provides the designer with the opportunity to easily examine the SCF with a dimensionless geometric parameter. In this context, in the following subheadings, SCF values will be calculated according to the appropriate β parameter and design curves will be created.

2.1. Design Curve Generation for Nozzle-Cylinder Junction Under Internal Pressure Loading

In that section, a cylinder of a prescribed finite size is taken into account. In other words, the cylinder diameter and wall thickness remain constant through all analyses. Nozzle thickness and diameter are variables in this analysis.

As can be seen in Figure 1, curves for 13 different d_i/D_i ratios are plotted. The curves consist of SCF results for ten different t/T ratios. t/T values start from 0.2 and continue up to 2.0 with a constant increment of 0.2 units. The lowest t/T is also associated with the highest SCF. Some points for t/T variations are marked on the $d_i/D_i=0.728$ curve in Figure 1. Additionally, since the diameter of the cylinder is fixed and the diameter of the nozzle is variable, the Attachment Parameter is represented as in the equation.

$$\beta = \frac{0.875d_o}{D_m} \tag{Equation 1}$$

When Figure 1 is examined, it will be seen that the increase in d_i/D_i causes an increase in SCF for the same t/T ratios. In addition, when each curve is evaluated within itself, it is noteworthy that the increase in t/T values follows a parabolic decrease in SCF. When the d_i/D_i ratio drops below 0.25, this parabolic downtrend becomes a more linear downtrend.

Another scenario that has been considered uses t/T as the primary variable. The proposed curves range from $t/T = 0.25$ to 2.50 and advance by 0.25 steps for each

curve. Each point on the curves indicates the change in d_i/D_i in this case when D_i and T values are fixed. SCF values were acquired for a total of 11 separate d_i/D_i ratios throughout the creation of each curve, with a 0.05 rise in the ratios at each point. In Figure 2, generated curves are displayed.

As shown in Figure 2, d_i/D_i values start from 0.1 and continue up to 0.6 in increments of 0.05. Considering that the shell diameter remains constant, an increase in nozzle diameter also causes an increase in SCF values. Otherwise, SCF values decrease when t/T increases because the increased nozzle wall thickness has a positive effect on strength.

In the third case, different parameters are used to regulate the t/T change. In any case, the d_m/D_m value is equivalent to the t/T value. A total of 9 different t/T cases are considered in this case. It should also be noted that the shell wall thickness (T) is constant, and variations are created to change the nozzle wall thickness (t). The SCF data from 5 distinct analyses are used to draw each curve. Each of these points represents the scenario where D/T starts from 10 and continues up to 50 in 10 increments. The outcomes are displayed in Figure 3.

According to Figure 3, each case's SCF curves follow the same general trend. However, as t/T grows, d_m/D_m will expand at the same pace, resulting in a nozzle opening that nearly exceeds the 0.5 shell's diameter. Since the maximum stress will rise as a result, S.C.F values also have a tendency to rise dramatically.

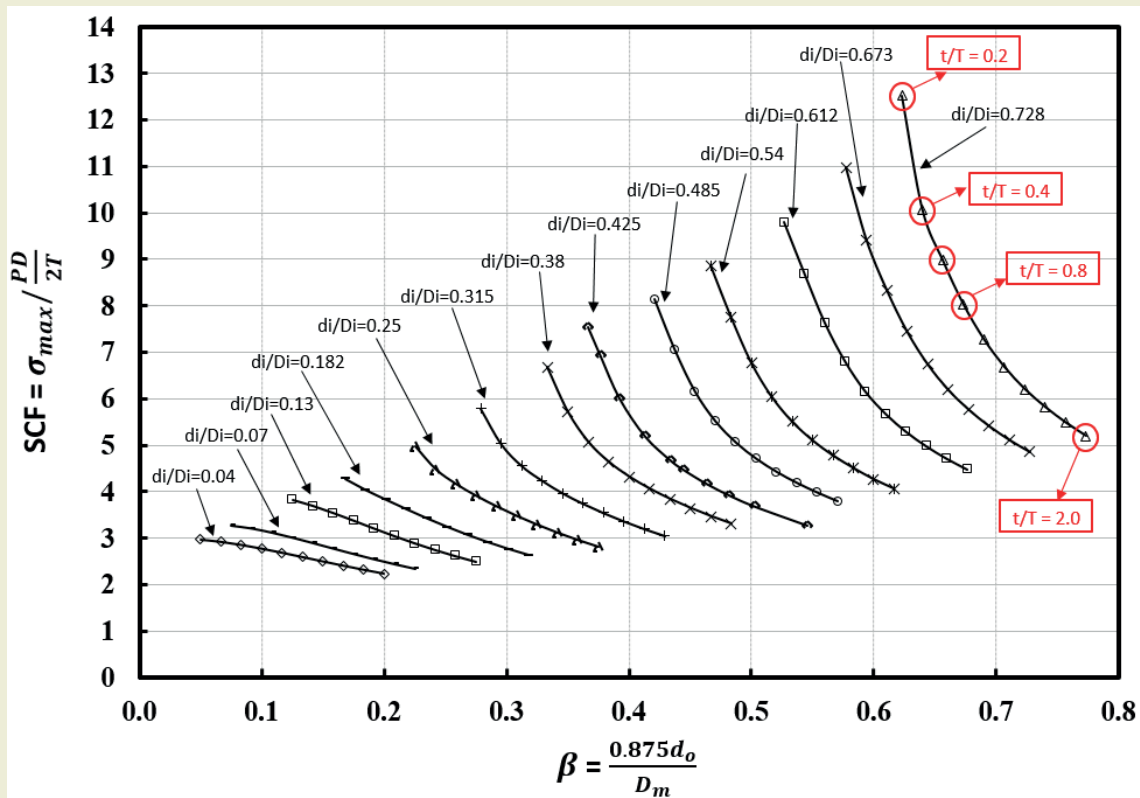


Figure 1. SCF Distribution for Nozzle/Cylinder Connection Under Internal Pressure – Without Pad Reinforcement (1st scenario)

When the $t/T = 0.15$ curve, in which SCF changes the least, the difference in the maximum SCF value is 21%. This difference occurs between the cases $D/T=10$ and $D/T=50$ where the first and last points are represented. When the $t/T=0.55$ situation, where the difference in the maximum SCF value is observed, is examined, it is seen that the proportional difference reaches 47%. In other words, it can be said that an approximately 3.5 times increase in t/T value corresponds to a 125% increase in SCF values.

For another case where the effect of the internal pressure

on the SCF distribution is examined, the D/T ratio is obtained from 10 to 50 with an increase of 5 units. By increasing the shell diameter (D) at a constant shell thickness (T), 9 different D/T values are created. Each D/T value represents a curve. These curves are formed by the parameter of d_m/D_m . The d_m/D_m changes are marked on the $D/T=10$ curve and all design curves are plotted in Figure 4. The t/T value was equal to 1 in all analyses. As shown in Figure 4, Although the nozzle diameter tends to increase at the same rate as the shell diameter, the change in SCF does not show the same trend. In the

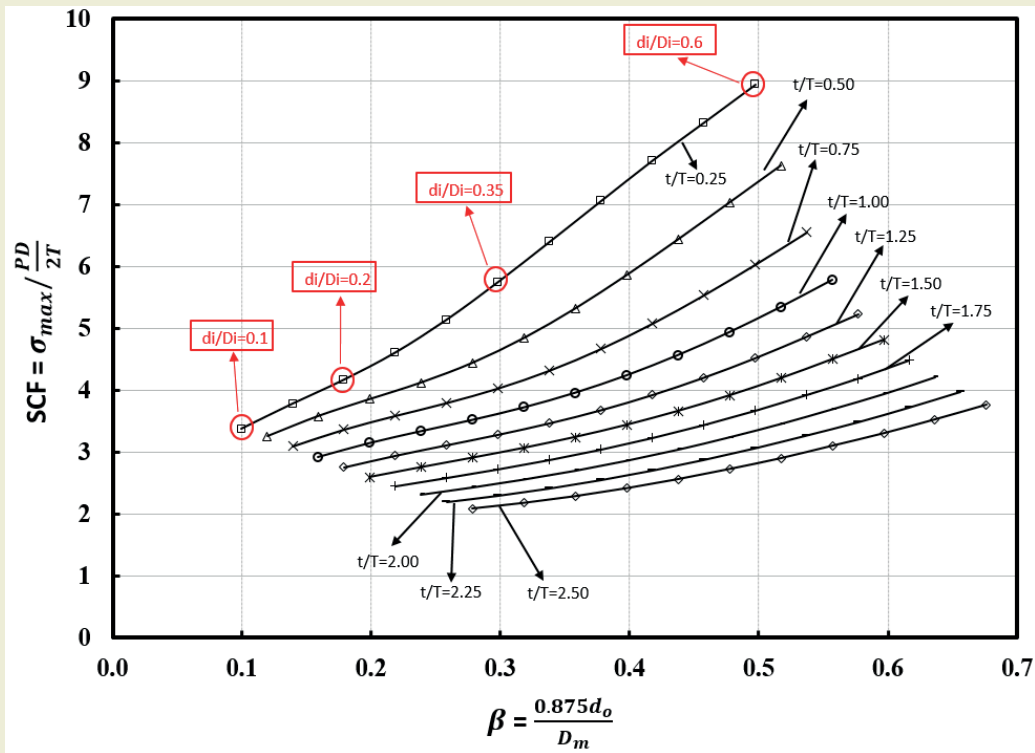


Figure 2. SCF Distribution for Nozzle/Cylinder Connection Under Internal Pressure – Without Pad Reinforcement (2nd scenario)

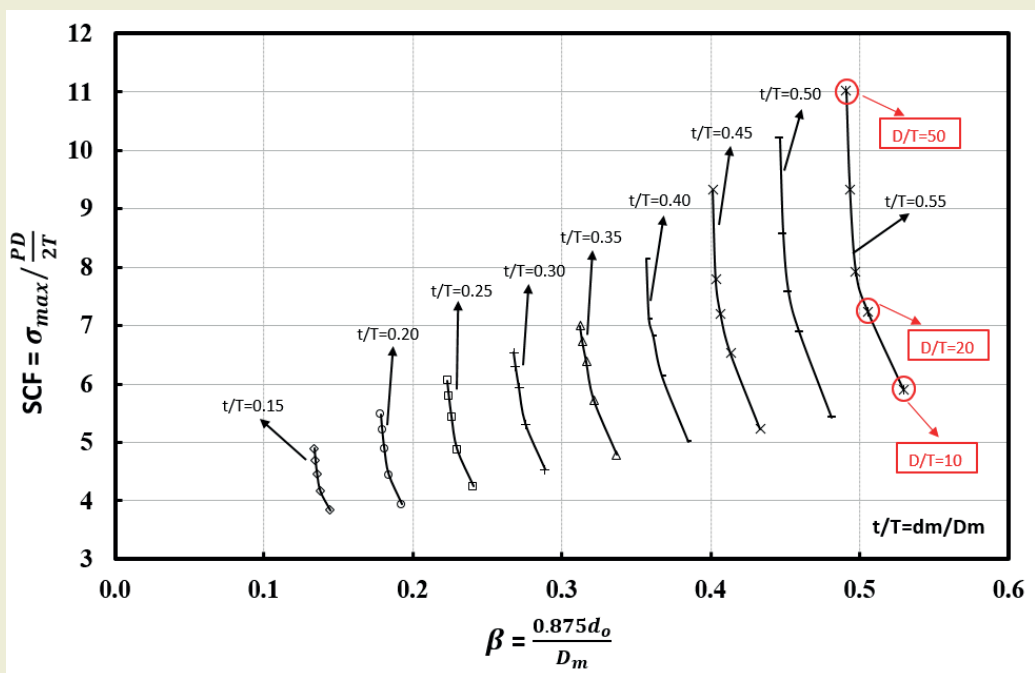


Figure 3. SCF Distribution for Nozzle/Cylinder Connection Under Internal Pressure – Without Pad Reinforcement (3rd scenario) ($t/T = d_m/D_m$)

case of this increase in dm/Dm of 0.15, it is just about 3% at its maximum point, and in the case of an increase in dm/Dm of 0.55, it is roughly 30%. All these results show that the larger the nozzle diameter, the linearly similar increase in SCF values.

2.2. Design Curve Generation for Nozzle-Cylinder Junction Under Internal Pressure Loading - Pad Reinforcement Effect

Reinforcement plate (pad) applications are one of the most effective ways to minimize the high stresses that

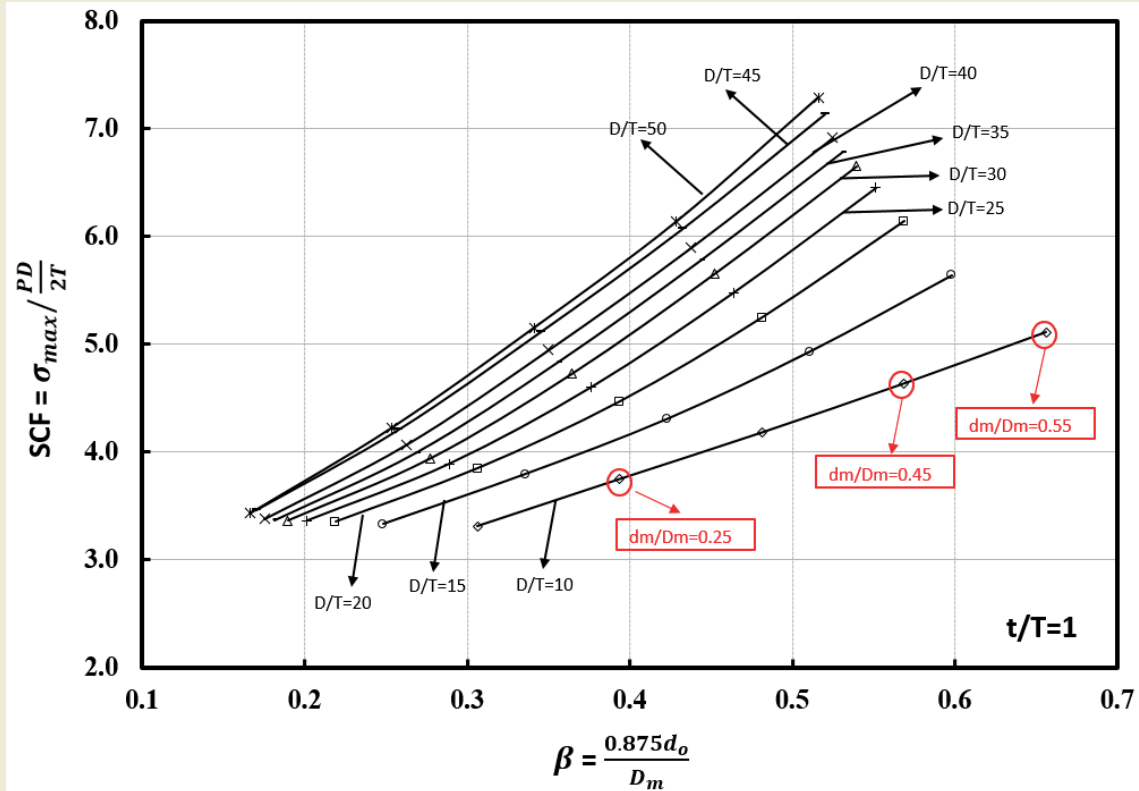


Figure 4. SCF Distribution for Nozzle/Cylinder Connection Under Internal Pressure – Without Pad Reinforcement (4th scenario) ($t/T = 1$)

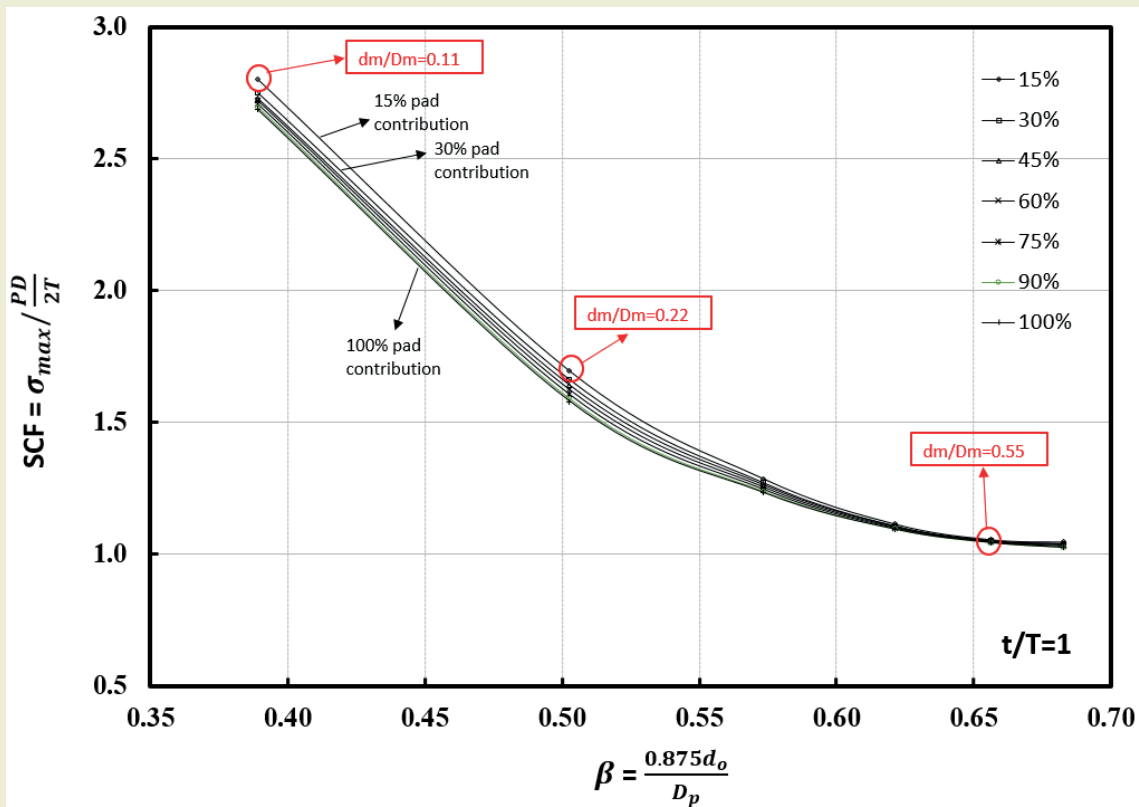


Figure 5. SCF Distribution for Nozzle/Cylinder Connection Under Internal Pressure – With Pad Reinforcement (1st scenario) ($t/T = 1$)

occur in pressure vessel problems. This application is conducted by adding additional material to the joint areas. In this section, it is discussed how the reinforcement plates added to the nozzle/cylinder connection regions will affect the Stress Intensity Factor magnitudes. In his paper, Stikvoort [19] presented a study of the effect of the geometric gap between a cylindrical or spherical shell and a reinforcement pad on the stress concentration near the nozzle penetration when the pressure vessel is subjected to internal pressure. The mentioned study is important for the stress magnitudes occurring between the nozzle and the reinforcement area. However, the focal point here is the maximum stress on the entire system, and this region occurs at the crotch corner. For this reason, the gaps between the pad and the main vessel are ignored and it is considered to be an integrated assembly.

First, a model with a constant t/T ratio of 1 is considered, and the pad thickness (T_p) is increased at regular intervals. Also, the dm/Dm ratio is increased by 0.11 with each step starting from 0.11 to 0.66. Here, the shell diameter (Dm) is fixed. The main variable is the nozzle diameter (dm). In Figure 5, generated curves are displayed.

Another scenario is that the pad reinforcement is the key variable in this case, so the attachment parameter - β is modified to account for the diameter of the pad. The new expression is;

$$\beta = \frac{0.875d_o}{D_p} \tag{Equation 2}$$

As seen in Figure 5, it can be said that pad reinforcement is more effective in reducing stress as the dm/Dm ratio

decreases, that is, the smaller the nozzle opening. This SCF change ratio remains below 1% after 0.44 dm/Dm . However, when dm/Dm is 0.11 the SCF difference shows a 4.21% decrease at the maximum point.

Increasing the pad thickness in an equivalent manner is one of the main variables that influence the effect of pad contribution on SCF change. Varying the pad diameter (D_p) is the other variable. Five different D_p/dm ratios are determined for each curve generation (1.25, 1.5, 1.75, 2.0, and 2.25) to observe the effect of this variable. During the analysis, the pad diameter (D_p) is increased at constant intervals while the nozzle diameter (dm) remains constant. The results are indicated in Figure 6.

Given that both the opening of the nozzle as well as the outside dimensions of the main cylinder do not change, it is clear that changing the pad diameter has a significant impact on the SCF as well. An increase in pad diameter of approximately two times will result in a decrease in SCF values of approximately 80% if $D_p/dm = 1.25$ is compared with $D_p/dm = 2.25$. A decrease in S.C.F values is also achieved by increasing pad thickness, in line with the previous graph. With a clearer expression, an 85% pad contribution will increase S.C.F by over 13% on average.

In this section, the effects of reinforcement plate application under various parameters were examined and design curves were created. Based on these results, it has been shown that pad reinforcement ratio and pad diameter have positive effects on reducing the stress concentration factor. However, it has been shown in the curves obtained that the reinforcement plate application will not

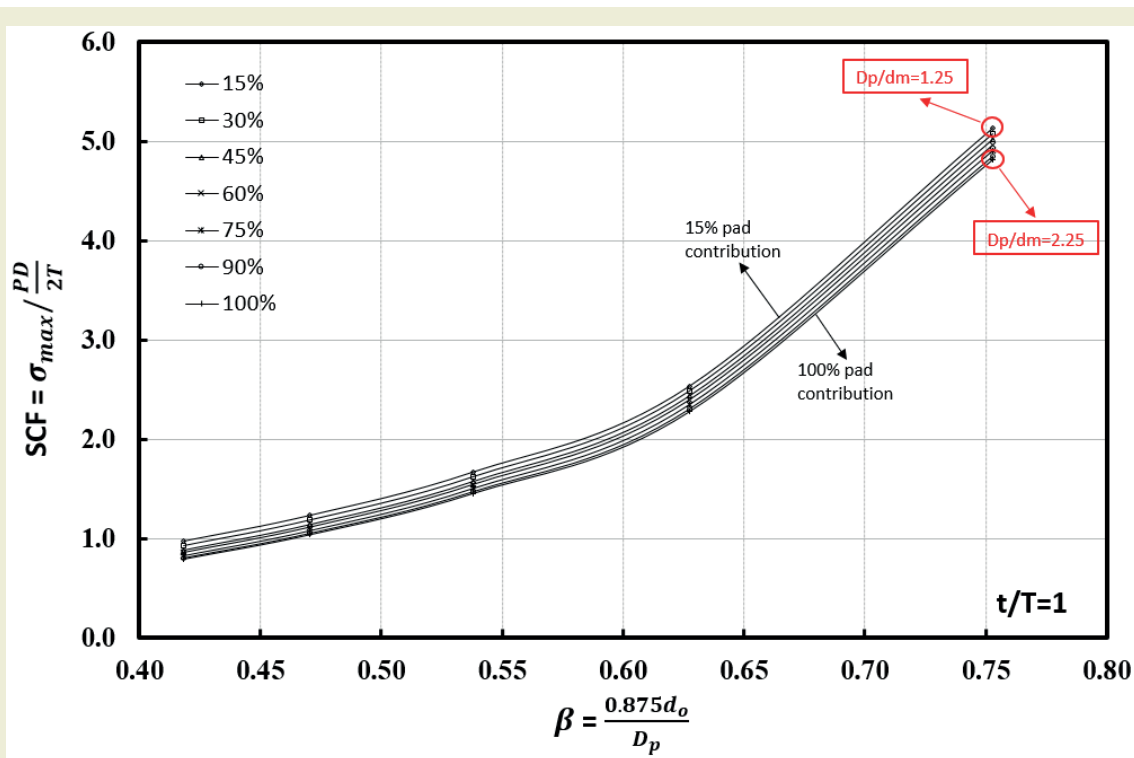


Figure 6. SCF Distribution for Nozzle/Cylinder Connection Under Internal Pressure – Without Pad Reinforcement (2nd scenario) ($t/T = 1$)

provide the desired performance if the nozzle opening is too large (especially if the d/D value is 0.5 and above). In such cases, it is stated that the pad diameter can be increased together with the pad thickness and the SCF could be reduced.

2.3. Design Curve Generation for Nozzle-Cylinder Junction Under External Local Loads

Following the above studies, the maximum stresses and stress concentration factors related to external local loadings are now determined. Thereafter, by using a suitable attachment parameter, design curves related to external loads are established. Since the stress results depending on the direction of the force will differ for the same load magnitudes in external local loadings, the SCF expression has been rearranged in Equation 3.

$$SCF = \sigma_{max} / \frac{V_i}{2\pi R t}, \quad (i = x, y, z) \quad \text{Equation 3}$$

In that formula, V_x , V_y , and V_z denote the shear force in the axial direction, the shear force applied in the longitudinal direction, and the tensile force, respectively. The aforementioned local loads are illustrated in Figure 7.

For all problems to which external loading will be applied, the mentioned loading conditions are exactly met. The d_i/D_i ratio is the main parameter for all analyses. Design curves are created for 11 different ratios of that parameter. Here, for the d_i/D_i parameter, it should be noted additionally, the value of D_i is constant in all cases. That means the size of the main shell does not change. In

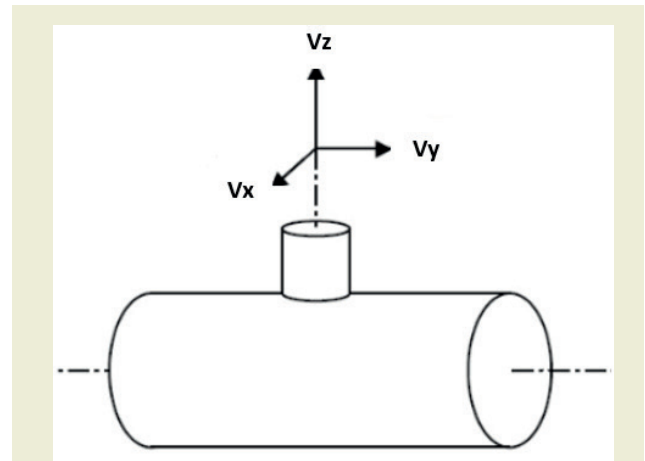


Figure 7 Loading states for nozzle/cylinder connections.

contrast, the nozzle inner diameter - d_i is increased with each step. Also, another parameter used to create the design curves is t/T . The t/T ratio is obtained for 10 different points in increments of 0.2 from 0.2 to 2.0. Choosing these variables in the design curve graph has the purpose of providing the possibility to examine the diameter and thickness of the nozzle and cylinder during the same parametric study, which directly affects the maximum stress that will be imposed on the structure.

The generated design curves are shown are demonstrated in Figure 8, Figure 9, and Figure 10.

As the t value increases up to the $d_i/D_i = 0.38$ curve in Figure 8, the SCF values decrease almost linearly. It is

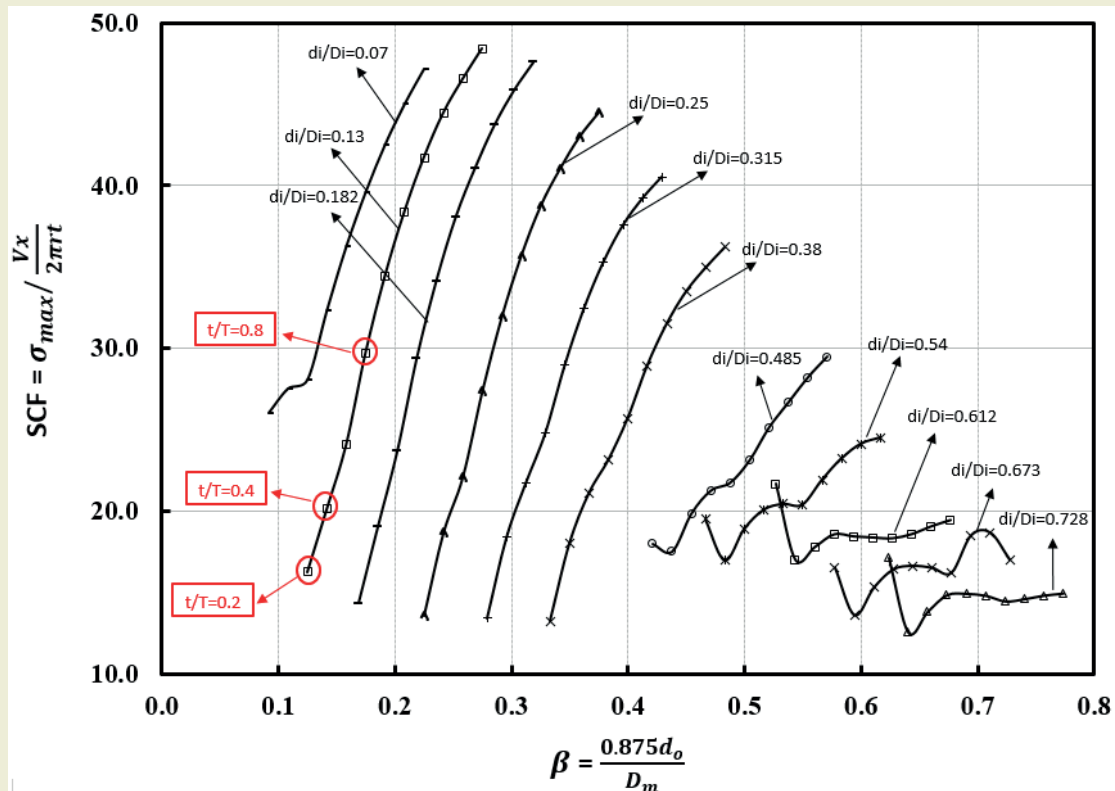


Figure 8 SCF Distribution for Nozzle/Cylinder Connection Under External Loads (V_x)

also striking that the SCF is remarkably high at the $t/T=0.2$ point. This point is also the $d_i/D_i = 0.485$ point, i.e., the nozzle radius is almost half the size of the cylinder radius. This shows that the increased shell diameter increases the stress magnitude and at this point, the nozzle wall thickness - t cannot meet the maximum stress. For this reason, the $t/T=0.2$ point for this Figure is the most striking point in the design curves obtained. It is also noted that the maximum SCF obtained for the same

t/T decreases with increasing nozzle inner diameters, and the wall thickness effect almost disappears.

When the cases where the V_y force is applied in Figure 9 are examined, it is seen that the interpretations that can be made for V_x in Figure 8 will be mostly similar. The progression of the curves, though, follows a similar trending pattern, especially after the $d_i/D_i=0.425$ curve, which is quite remarkable. On the contrary, in the case

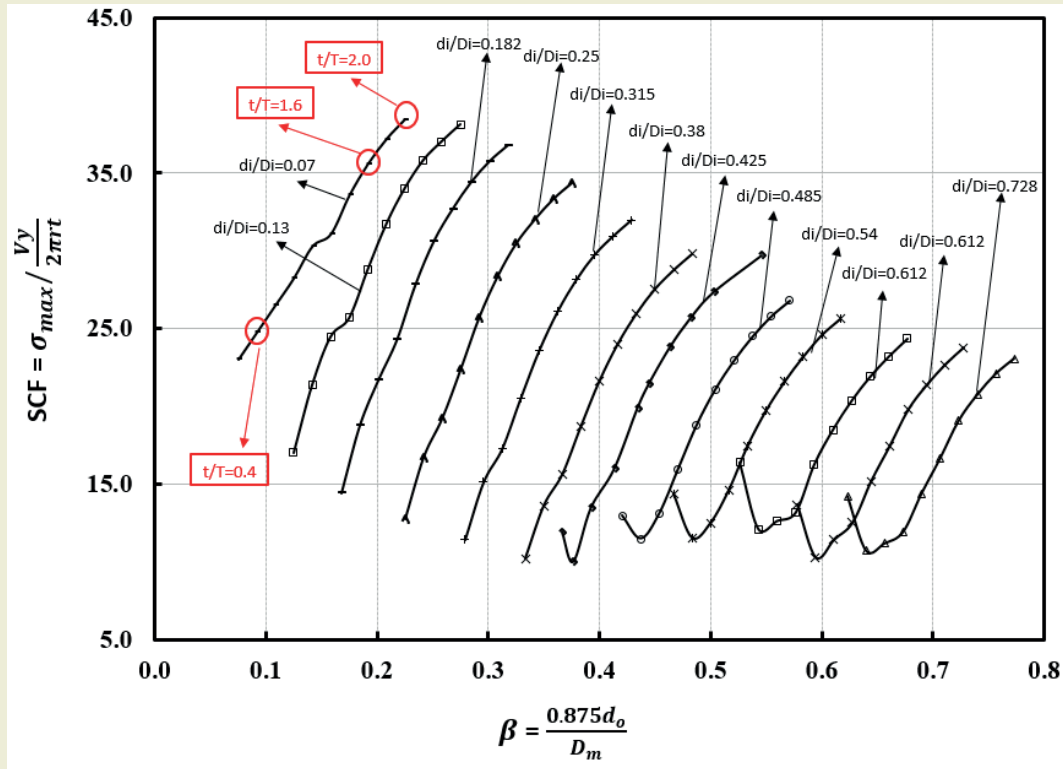


Figure 9. SCF Distribution for Nozzle/Cylinder Connection Under External Loads (V_y)

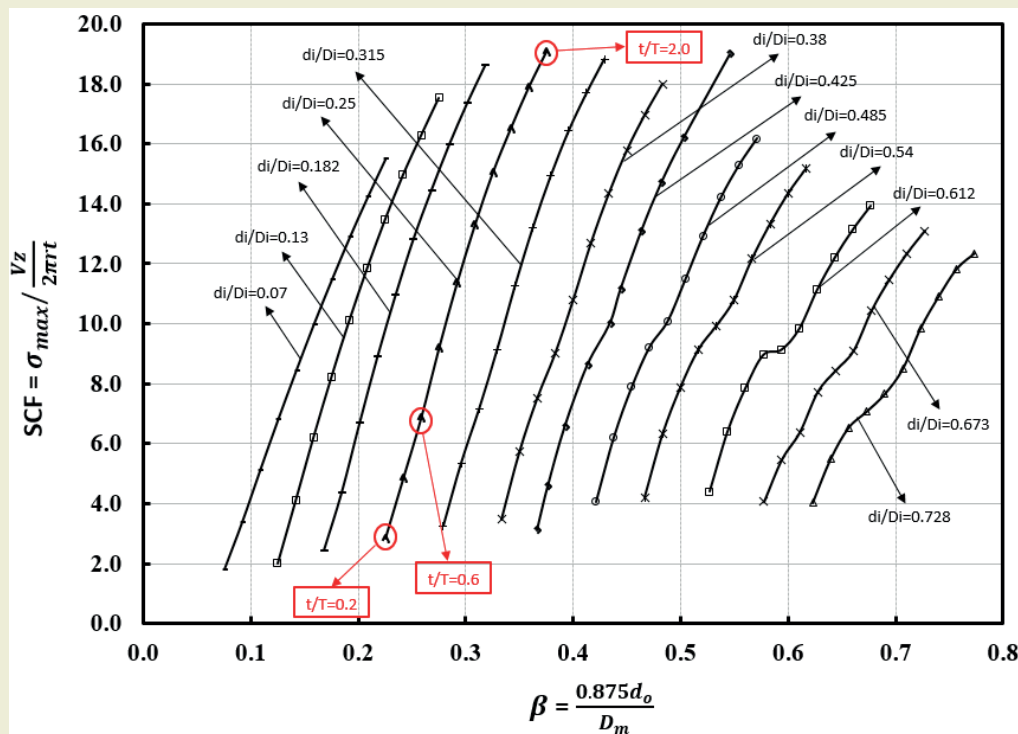


Figure 10. SCF Distribution for Nozzle/Cylinder Connection Under External Loads (V_z)

of $t/T=0.2$, the nozzle wall thickness is not able to meet the loads on the structure, and there is too much stress observed on the wall. Additionally, it is worth noting that if V_x loading is performed, SCF values tend to be 15% higher on average compared to V_y loading. As a result, the system is often subjected to greater force in the X direction than in the longitudinal direction when applying axial loading.

The case of loading in the Z direction (tensile load) is the last loading condition to be examined. The outcomes are displayed in Figure 10. The SCF will increase in value if it is increased as it is in any other external load when each curve is examined separately.

3. Conclusions

It is concluded that the maximum stresses calculated by FEA and SCF are obtained for the cylinder/cylinder joints under the influence of internal pressure and external local loads. From this, different parametric approaches and loading conditions were applied to the basic dimensions

of geometry. There were also a number of design curves for cylinder-to-cylinder connections created. In all cases where design curves have been obtained, it can be seen that pressure and external loads are both responsible for a non-linear relation between load and stress. It is also of significance to note that the analysis made in this case, and the curves obtained, are only applicable to loads that operate in a one-way direction (tensile, longitudinal, and axial loading separately, etc.). In conclusion, this paper provides designers and researchers with useful guidelines for calculating parameters related to thickness and diameter under external load and internal pressure conditions.

In conclude, it is exceedingly difficult to define a single formulation for the obtained design curves due to the fact that they contain a complex number of variables and parameters. As such, by using the approach presented herein, by combining appropriate parameters, equations suitable for finite element analysis can be developed in future studies.

References

- [1] Leckie, F. A., & Penny, R. K. (1963). Stress Concentration Factors for the Stresses at Nozzle Intersections in Pressure Vessels (Welding Research Council Bulletin 90).
- [2] Spence, J., & Tooth, A. S. (Eds.). (2012). Pressure vessel design: concepts and principles.
- [3] Kharat, A. R., Kamble, S. B., Patil, A. V., & Burse, I. D. (2016). comparative study of different approaches to estimate SCF in pressure vessel opening. *Int. J. of Mechanical Engineering and Technology*, 7: 142-155.
- [4] Money, H. A. (1968, January). Designing flush cylinder-to-cylinder intersections to withstand pressure. In *Mechanical Engineering* 90(11): 74.
- [5] Moffat, D. G., Mwenifumbo, J. A. M., Xu, S. H., & Mistry, J. (1991). Effective stress factors for piping branch junctions due to internal pressure and external moment loads. *The Journal of Strain Analysis for Engineering Design*, 26(2): 85-101.
- [6] Moffat, D. G., Mistry, J., & Moore, S. E. (1999). Effective stress factor correlation equations for piping branch junctions under internal pressure loading. *Journal of Pressure Vessel Technology*, 121(2): 121-126
<https://doi.org/10.1115/1.2883674>
- [7] Mershon, J. L. (1987). Local Stresses in Cylindrical Shells due to External Loadings on Nozzles? Supplement to WRC Bulletin No. 107 (Revision 1). WRC Bulletin.
- [8] Lind, N. C. (1968, January). Approximate stress-concentration analysis for pressurized branch pipe connections. In *Mechanical Engineering* 90(3): 78
- [9] Decock, J. (1975). Reinforcement method of openings in cylindrical pressure vessels subjected to internal pressure. *Weld. Res. Abroad*, 21(9): 9-36.
- [10] Kihui, J. M., Rading, G. O., & Mutuli, S. M. (2007). Universal SCFs and optimal chamfering in cross-bored cylinders. *International journal of pressure vessels and piping*, 84(6): 396-404.
- [11] Mukhtar, F. M., & Al-Gahtani, H. J. (2019). Comprehensive Evaluation of SCF for Spherical Pressure Vessels Intersected by Radial Cylindrical Nozzles. *International Journal of Steel Structures*, 19: 1911-1929.
- [12] Gerdeen, J. C. (1972). Analysis of stress concentrations in thick cylinders with sideholes and crossholes. *Journal of Manufacturing Science and Engineering*, 94(3): 815-824
- [13] Nziu, P. K., & Masu, L. M. (2019). Offsetting of circular cross bore effects on elastic pressurized thick cylinders. *International journal of mechanical and production engineering research and development*, 9: 71-82.
- [14] Makulsawatudom, P., Mackenzie, D., & Hamilton, R. (2004). Stress concentration at crossholes in thick cylindrical vessels. *The Journal of Strain Analysis for Engineering Design*, 39(5): 471-481.
- [15] Kharat, A., & Kulkarni, V. V. (2013). Stress concentration at openings in pressure vessels-A review. *International Journal of Innovative Research in Science, Engineering and Technology*, 2(3): 670-678.
- [16] Bozkurt, M. (2022). Towards a unified design-by-analysis solution to pressure vessel nozzle-shell junctions under combined loading, PhD, University of Strathclyde Engineering, UK
- [17] Bozkurt, M., Nash, D., & Uzzaman, A. (2021). A comparison of stress analysis and limit analysis approaches for single and multiple nozzle combinations in cylindrical pressure vessels. *International Journal of Pressure Vessels and Piping*, 194: 104563.
- [18] Bozkurt, M., Nash, D., & Uzzaman, A. (2020, October). Effect of the internal pressure and external loads on nozzles in cylindrical vessel. In *IOP Conference Series: Materials Science and Engineering*, 938(1): 012007.
- [19] Stikvoort, W. (2021). Effectiveness of reinforcement plates pertaining to pressure equipment. *American Journal of Engineering Research (AJER)*, 10(8): 127-146.

4. APPENDIX

Notation

d_i : nozzle inner diameter

d_o : nozzle outer diameter

d_m : nozzle mean diameter

D_i : shell inner diameter

D_o : shell outer diameter

D_m : shell mean diameter

D_p : pad diameter

FEA: Finite Element Analysis

FEM: Finite Element Modelling

SCF: Stress Concentration Factor

t: nozzle thickness

T: shell thickness

β : attachment parameter